# Mechanistic Understanding of Line End Shortening

Michael D. Stewart*, Gerard M. Schmid, Sergei V. Postnikov†, C. Grant Willson
Dept. of Chemical Engineering, The University of Texas at Austin
Austin, TX 78712

## ABSTRACT

In recent years the line end shortening (LES) phenomena, known also as line end pullback, has emerged as a significant issue in microlithography. The causes of LES include aerial image formation, simple pattern geometry considerations, and diffusion effects. This paper presents an overview of the main causes of LES with particular attention to contributions due to exposure gradients at the feature edge. The effect of exposure gradients on acid diffusion is described and results of experiments designed to study gradient effects are presented along with simulation of diffusion contributions to LES. Simulation and experiment suggest that transport-related resist bias mechanisms affect LES in complex ways. In addition to diffusion simulations, aerial image calculations are presented as simple demonstration of the contribution of the imaging system to LES.

**Keywords:** acid diffusion, line end pullback, line end shortening

## 1. INTRODUCTION

Line end shortening (LES) has emerged as a serious problem in microlithography. LES can be overcome simply by biasing the mask dimensions, that is making the mask line longer relative to the desired printed length, but this limits achievable circuit density. Optical proximity correction (OPC) can also be used, but compensating for LES in mask design is complicated by the fact the causes of the LES phenomenon are poorly understood. This paper attempts to separate the causes of LES into individually understandable mechanisms that can eventually be recombined in lithography simulation programs. The main contributions to LES can be divided into optical effects, geometry effects, and diffusion effects. This paper will address each of these contributors and will also provide an experimental study of diffusion effects.

### 1.1 Optical Effects

A significant portion of the LES problem is the result of aerial image formation. When an imaging system is operated near its resolution limit, the physics of diffraction dictate that narrow lines show LES if printed to mask width. Even large features experience corner rounding as the higher order information about the pattern is lost in diffraction. Figure 1 shows the aerial image of an isolated line end simulated in PROLITH™ with the mask pattern overlaid in outline form. This aerial image demonstrates the problem; a line with dimensions near the resolution limit of the imaging system cannot simultaneously be printed to both the mask width and the mask length. Clearly, there can be a significant LES problem prior to the image even being deposited into the photoresist. In addition there is no obvious way for the photoresist to compensate for this problem. Even a perfect threshold-switching, no bias photoresist could only replicate the iso-energy profiles of the available aerial image.

While this aerial image line shortening is really unavoidable when operating near the diffraction limit, OPC enhancements and other imaging "tricks" can work to mitigate the problem. Improving resolution by moving to smaller $\lambda$ or higher numerical aperture will also improve LES for a given feature dimension, but this is equivalent to moving away from the diffraction limit. A fuller description of the optical causes of LES and how optical system parameters affect LES can be found in the work of Mack.[1, 2] An experimental investigation of the relationship between imaging system parameters and LES has also been reported by Shi *et al*.[3]

---

[*] Email: *stewart@che.utexas.edu*

[†] Currently at Motorola, Inc. Austin, TX

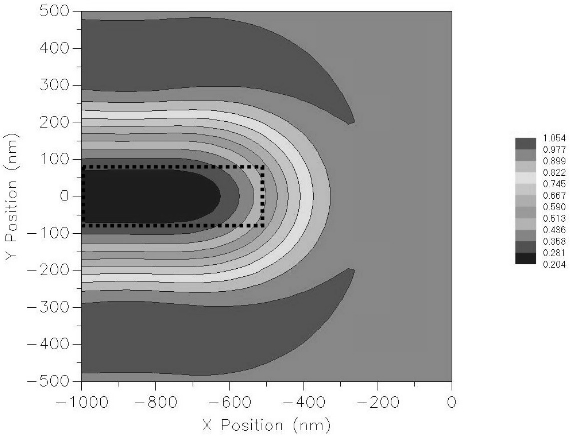

**Figure 1**: PROLITH simulated aerial image of 150nm isolated line end. Outline of mask is overlaid. ($\lambda$=248nm,$\sigma$=0.5, NA=0.5)

### 1.2 Feature Geometry Effects (Shape Considerations)

Even if a perfectly modulated image could be deposited into the photoresist (say by contact printing) LES could still be problem. At feature corners, diffusion of photoproducts from multiple directions works to round corners. If diffusion lengths at corners are sufficient to overlap adjacent corners, corner rounding becomes line end shortening. Differences in LES distances based on pattern shape have been reported in the work of Cheng et al.[4] In Cheng's work it was found the post exposure bake simulator STORM did not fully capture the effect of multi-dimensional diffusion as it underestimated the actual diffusion distances for 2-D mask patterns such as posts.

Diffusion from multiple directions can greatly enhance the photoproduct diffusion distances and must be accounted for to accurately predict lithography results. Fortunately, textbook diffusion analysis can be used to predict 2-dimensional diffusion distances in many cases. In 2-D diffusion two general cases are possible: convergent and divergent. In the convergent case the unexposed region is more or less surrounded by exposed regions. In the divergent case the opposite is true. In the positive tone, convergent cases include printing of a post and the printing of a line end. Divergent cases in positive tone include printing of a contact hole and the inside corner of an elbow.

The difference between convergent and divergent cases can be seen clearly in the printing of posts and holes. Figure 2 shows the initial and final conditions of a post (unexposed in the center) and hole (exposed in the center), the overlaid arrow indicates the general direction of diffusion. Finite element analysis incorporating Fickian diffusion equations was used to determine photoproduct movement over the course of a PEB. The diffusion coefficient was set to $10^{-5}$ $\mu m^2/s$.

Figure 3 plots the movement of an arbitrary concentration (30% of initial concentration) contour. Assuming a threshold development model (threshold = 0.3), the absolute change in radius is plotted for both the post and the hole case shown in Figure 2. The decrease in radius of the post is much greater in extent and faster than the increase in radius of the hole. In fact in this case the post would completely disappear over the course of the PEB. This effect can be explained by simple volumetric arguments. For a given change in radius the increase in occupied volume is less for the post than for the hole, and thus the photoproduct concentration dies out more slowly. A line end, especially with rounded corners from the aerial image, can be thought of as sort of half post, which leads directly to the expectation that diffusion will shorten the line by more than the one-sided line width bias distance.

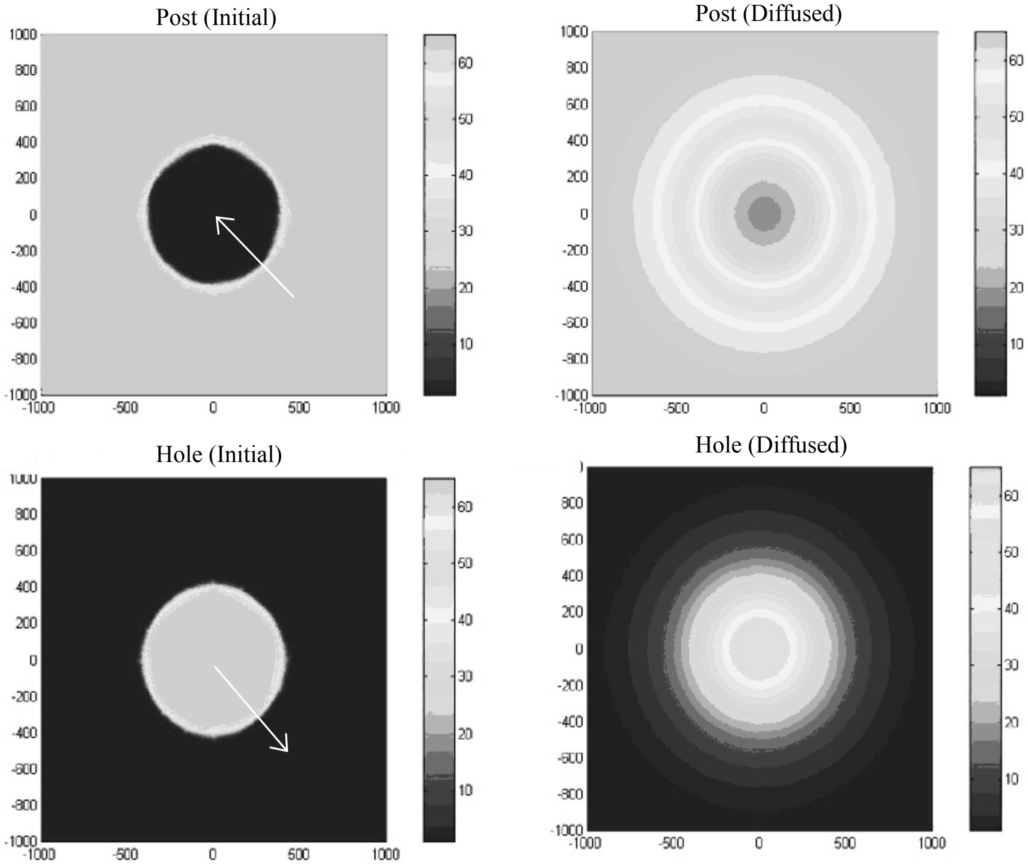

**Figure 2:** Diffusion simulation of post and hole exposure cases. Lighter regions correspond to higher acid concentrations.

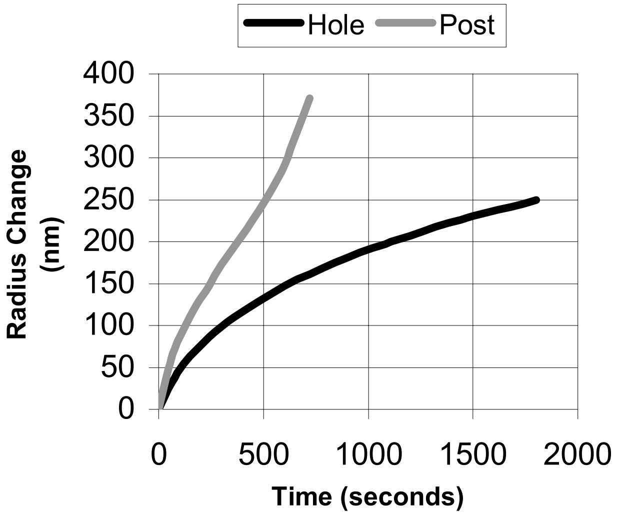

**Figure 3:** Plot of absolute radius change vs. time for post (convergent) and hole (divergent) diffusion cases.

### 1.3 Diffusion Effects

Analysis in the previous section assumed diffusion of photoproducts obeyed simple Fickian diffusion rules, that is the photoproducts and the photoresist matrix resin were non-reactive. This is the case in non-chemically amplified system like novalac/DNQ I-line resists, but in chemically amplified systems the diffusing species is a photogenerated acid that catalyzes reactions as it moves through the matrix resin. As a result acid transport occurs by a coupled reaction-diffusion mechanism which complicates analysis. Our research group has previously proposed a transiently enhanced reaction-diffusion mechanism to explain observed experimental results.[5, 6] In this model, as acid diffuses it catalyzes the deprotection reaction of blocked polymer sites and locally promotes its own diffusive mobility. This mobility enhancement is a by-product of the deprotection reaction that converts insoluble regions into soluble regions. Mobility enhancement can result from an increase in matrix resin free volume or from resin plastization as deprotection reaction by-products, like carbon dioxide and isobutylene, are generated in the film. If the enhancement to mobility were permanent the reaction-diffusion system could be modeled as Case II Fickian diffusion, as has been proposed by Zuniga *et al.*[7] But in reality the enhancement is not permanent, as the gaseous products appear to quickly desorb from the film and the generated free volume does not permanently remain.[8]

An additional complication to reaction-diffusion analysis is the presence of exposure gradients at the feature edge. These gradients arise due to diffraction and cannot be avoided in conventional lithography. This exposure gradient in turn generates a gradient of acid concentration. Another factor complicating analysis is that the slope of concentration gradients at the line end can be different from the slope at the line edge. Shown in Figure 4 is the exposure intensity versus position for the indicated crosscuts on an isolated line end aerial image, corresponding to the line end and line edge. Note that the aerial image slope is shallower at the line end than at the line edge

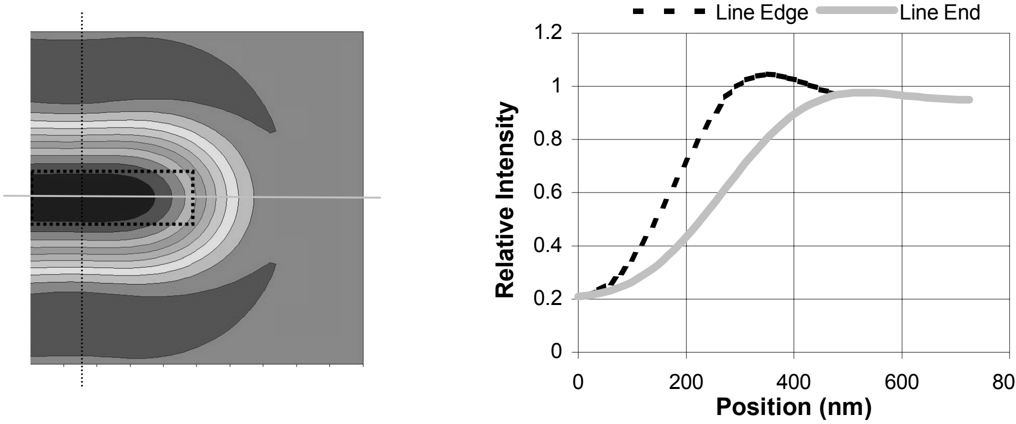

**Figure 4:** Aerial image of isolated line end. Intensity profiles are shown for indicated crosscuts at the line edge and line end. (nominal feature width: 150nm, $\lambda$=248nm,$\sigma$=0.5, NA=0.5)

Acid gradients can affect the reaction-diffusion system in two ways. A shallow acid gradient means there is less need for diffusion; that is, higher levels of acid are already present ahead of the threshold acid concentration front so less total movement of acid is required. The effect of these low levels of acid reacting while waiting for the threshold acid concentration levels to arrive also needs to be considered. As the acid reacts prior to the arrival of the threshold front, it removes matrix reactivity. Removing matrix reactivity removes mobility enhancement opportunities. In a sense there are competing mechanisms - less diffusion is required, but less mobility is available. On first consideration it is not clear which effect will dominate.

Experiments were devised to separate these two competing effects. Instead of studying a full gradient spectrum at once, it was decided to divide the gradient into discrete pieces and test individual concentration “slices”. Concentration in the gradient slice can then be varied in the experiment and the results combined to give information about the entire gradient. For studying the effect of concentration enhancement (i.e. acid present ahead of the threshold front) a bilayer polymer film stack experiment was used. One layer of the bilayer acts as a high acid concentration feeder layer while the other layer models the gradient slice. To model the gradient slice, acid concentration was varied in the upper, reactive layer by varying initial photoacid generator loadings. Measurement of the threshold front's diffusion distance was carried out using a scanning electron microscope after applying a silylation-based staining technique to the wafer cross-section. Experiments designed to investigate the reaction depletion effect were also based on a bilayer technique. The same high acid concentration feeder layer was used, but instead of varying slice acid concentration the blocking ratio of the upper resist polymer was varied. Different copolymer ratios, vary from 15% blocked to 100% blocked, were synthesized. A FT-IR based analysis was used to evaluate acid transport distances.

These individual experimental results can be used as inputs into or checks on reaction-diffusion models. In effect simulation can be used to reconcile the two effects that were separated in experimental design. Results from a mesoscale reaction-diffusion simulator that incorporates the transiently enhanced diffusion model are shown in a subsequent section. Simulation is shown to match the trends observed experimentally.

## 2. EXPERIMENTAL

Copolymers of 4-tert-butyloxycarbonyloxystyrene (TBOC) and 4-hydroxystyrene (PHS) were prepared by partial thermolysis of TBOC homopolymer. The homopolymer, poly(4-tert-butyloxycarbonyloxystyrene) (PTBOC), was prepared by free radical initiated polymerization of TBOC monomer supplied by TriQuest Chemical. Azobisisobutyronitrile (AIBN) initiator in 150:1 mole ratio (monomer:initiator) was used and the polymerization was carried out at 70 ºC for 18 hours in toluene solvent. Resulting polymer was precipitated into petroleum ether and collected by filtration. Heating of the TBOC polymer powder to 160 ºC in a Kugelrohr (Buchi) for varying lengths of time caused some fraction of the TBOC units to convert into PHS units. By varying heating times, different ratios of protected and unprotected sites were obtained. Copolymer ratios were determined by thermogravimetric analysis and confirmed by IR analysis. It has been reported[9] that the thermolysis reaction that converts TBOC units into PHS units does not proceed perfectly cleanly in the solid state, but rather various by-products are also produced in small amounts. This thermolysis approach to copolymer synthesis captures the effect of the side reaction products on polymer transport properties where as other synthetic approaches would not.

The photoacid generator (PAG) used in these experiments was bis(p-tert-butylphenyl)iodonium perfluorobutanesulfonate, also known as a "nonaflate". Polymer film stacks were formed by floating techniques described in previous work.[5] Acid feeder layers consisting of poly(4-methoxystyrene) with a 5 wt% (dry) PAG loading were spin cast onto silicon wafers from propyleneglycol methyl ether acetate (PGMEA). These feeder layers were approximately 300 nm thick after a 120 second, 90 ºC post apply bake (PAB). For the first series of experiments the top films in the bilayer stack were PTBOC with a varying PAG loading. PTBOC films were approximately 600 nm thick after processing. In the second set of experiments the upper films were copolymers of TBOC and PHS with a varying TBOC:PHS ratio. These copolymer films were floated from sodium chloride crystals and were approximately 300 nm thick after processing. Figure 5 depicts the two different layer constructions used in these experiments. Completed film stacks were exposed to a 248 nm wavelength dose of approximately 90 mJ/cm$^2$ prior to the PEB step. The full details of the SEM silylation staining technique used to visualize acid diffusion and the FT-IR analysis technique are reported elsewhere.[5, 6]

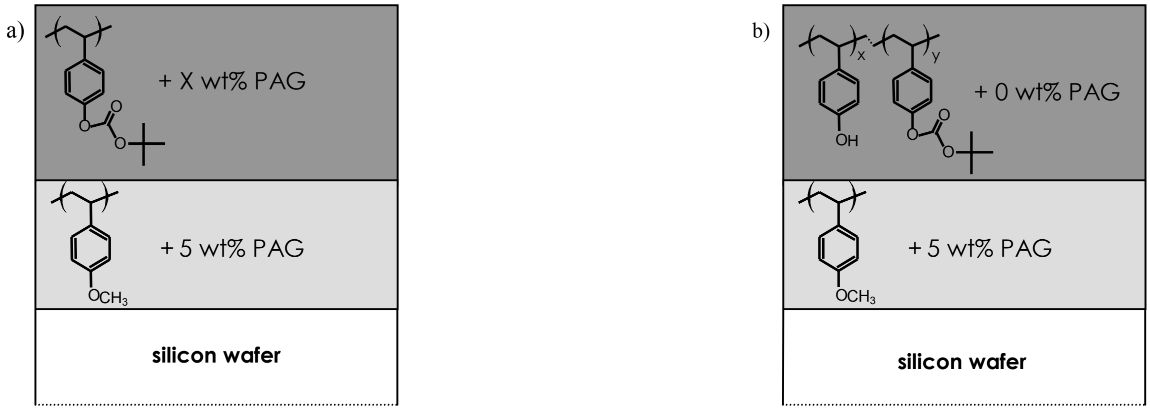

**Figure 5:** Layer construction for a) the concentration enhancement experiment b) the reaction depeletion experiment. In 5a PAG concentration (X) in the upper layer varies while in 5b the x:y copolymer ratio between PHS and TBOC varies.

## 3. EXPERIMENTAL RESULTS

### 3.1 Concentration Enhancement

By varying acid concentration in the upper (TBOC) layer and then measuring the width of the fully deprotected region, the effect of having acid ahead of the threshold front can be seen. PAG loadings in the upper layer were set at 0 wt%, 0.16 wt%, 0.26 wt%, and 0.40 wt%. These weight percent loadings correspond to mole ratios (PAG to monomer unit) of 0 to 1, 1 to 1200, 1 to 800,and 1 to 300, respectively. Measured results correspond to expectations: upon exposure, higher PAG loadings lead to more deprotection and the threshold front moves further into the resist layer. Figure 6 below shows typical scanning electron micrographs of silylation-stained layer cross-sections obtained in this experiment. Bands visible in these micrographs are, from bottom to top, the silicon wafer, the acid feeder layer, fully silylated region, followed by partially silylated regions and unreacted regions. Unreacted regions near the top of the resist are the result of atmospheric base contamination levels which are present in the non-clean room environment where the samples were processed. In the case of the 0.40 wt% loading, nearly complete deprotection was observed throughout the upper layer. This suggests that the threshold acid concentration is between 0.40 wt% and 0.26 wt%. Measured distances for these four cases are presented in Table 1 below.

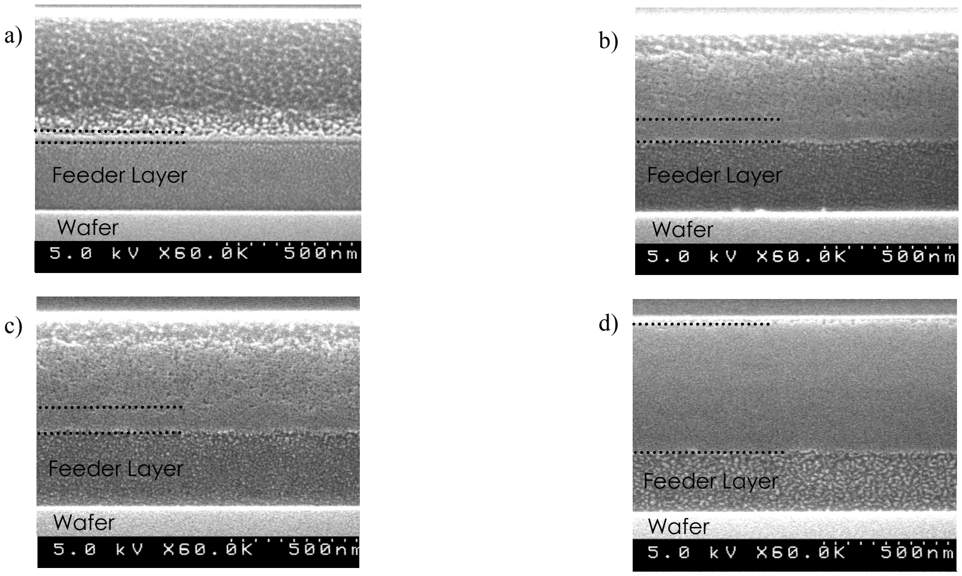

**Figure 6:** Scanning electron micrographs depicting the diffusion distance of a threshold front. Top layer TBOC with PAG loading of: a) 0 wt%, b) 0.16 wt%, c) 0.26 wt%, d) 0.40 wt%

**Table 1:** Summary of SEM experimental data

| PAG Loading in tBOC | Mole Ratio (TBOC:Acid) | Diffusion Distance |
|---|---|---|
| 0 wt% | 1:0 | 50nm |
| 0.16 wt% | 1200:1 | 100nm |
| 0.26 wt% | 800:1 | 110nm |
| 0.40 wt% | 300:1 | Full Reaction |

Concentration enhancement effects are clearly present, but the difference in acid concentration between negligible deprotection and full deprotection is small. Measuring differences in effects of minutely different acid concentrations is difficult due to process variations inherent in working outside a chemically filtered clean room environment. Minor acid concentration differences can have large effects, but environmental base contamination swamps attempts to finely adjust acid concentration.

### 3.2 Reaction Depletion

By varying the concentration of reactive sites in the upper layer and monitoring disappearance of an IR absorption band characteristic of the reactive species, acid diffusion distance can be determined as a function of copolymer blocking fraction. Lowering the blocking fraction is equivalent to depleting reactive sites available in the resist. Polymers with blocking fractions of 100%, 90%, 80%, 50% and 15% were prepared. Figure 7a presents the results of the IR experiments. IR absorbance data can be converted into acid diffusion distances if the initial layer thickness is known and it is assumed that reaction is confined to a reasonably sharp band. Diffusion distance are for a 90 ºC PEB. Figure 7b presents diffusion distances as a function of blocking fraction for a fixed PEB of 90 seconds. The effect of blocking fraction on diffusion distance is quite pronounced when going from 100% to 90% or 80%, but eventually this observed effect levels out somewhat. For example, decreasing blocking from 80% to 15% decreases the measured diffusion distance by less than 10 nm.

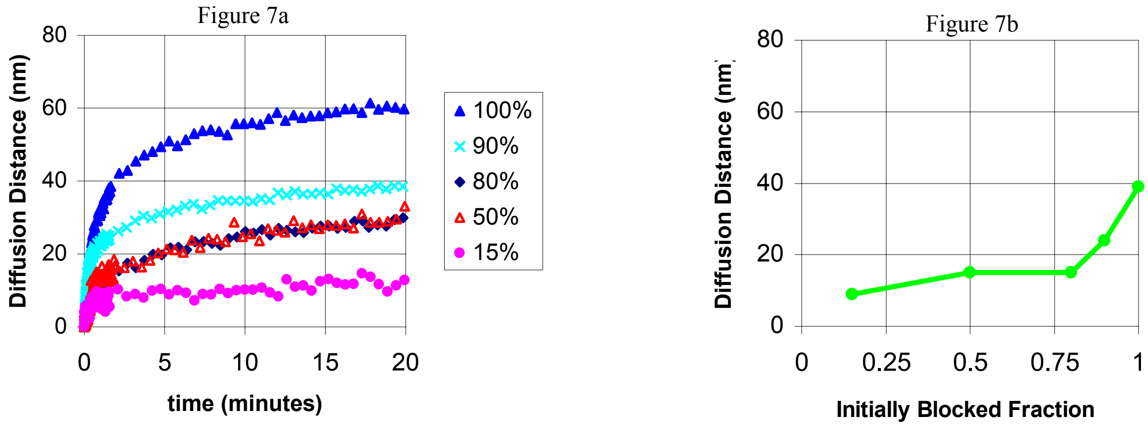

**Figure 7:** a) FT-IR traces of reaction progress in bilayer experiments (T = 90 ºC) with various blocking of the upper layer. b) Blocking fraction vs. diffusion distance after a 90 second/ 90 ºC PEB.

## 4. SIMULATION RESULTS

The experiments described above were designed to separate competing mechanisms so that individual mechanism might be understood. However, in actual systems of concern both mechanisms are operative simultaneously, and full understanding of the system requires knowledge of the interplay between all mechanisms present. But once individual mechanisms are understood, simulation provides a convenient way to combine multiple effects in a coherent way.

Our research group has been working towards lithography simulation from a mesoscale level.[10, 11] Our mesoscale approach takes the base unit for modeling consideration as the polymer repeat unit. When each repeat unit is considered separately, stochastic effects found in acid generation and diffusion are not smoothed out in simulation, as happens when the photoresist is approximated as a continuous medium. As feature sizes decrease eventually these stochastic effects will become a significant consideration in semiconductor manufacturing.

Two sets of simulation results are presented to demonstrate that the simulation captures the trends observed in experiment. Only initial conditions vary between the two simulations sets; all other modeling parameters are constant. In the following simulations each polymer repeat unit and acid molecule is considered individually, and the randomness of acid diffusion is apparent. A discussion of how this randomness affects properties such as line edge roughness (LER) is found elsewhere.[11]

### 4.1 Concentration Enhancement

Results of simulations designed to model the concentration effect are shown in Figure 8. These results show the interface of protected and deprotected regions, with light regions indicating a high concentration of blocking sites.

Figure 8a is the control case in which no acid is present in the upper layer of the film stack. In Figure 8b acid is present in the upper layer at a mole ratio of 1:800. In the control case the limit of deprotection is approximately 30 nm from the layer interface. This is in comparison to the experimentally SEM-measured value of approximately 50 nm. In the simulated case of acid being present ahead of the main acid front deprotection is seen through out the entire simulated thickness of 80 nm. These results are in general agreement with the experimental results. Due to limitations in simulation construction, the blocking fraction of the upper layer is limited to a maximum of about 80%. As a result, the simulated cases are not perfect analogs of the experiments as the upper layer in the SEM experiment was fully (100%) protected.

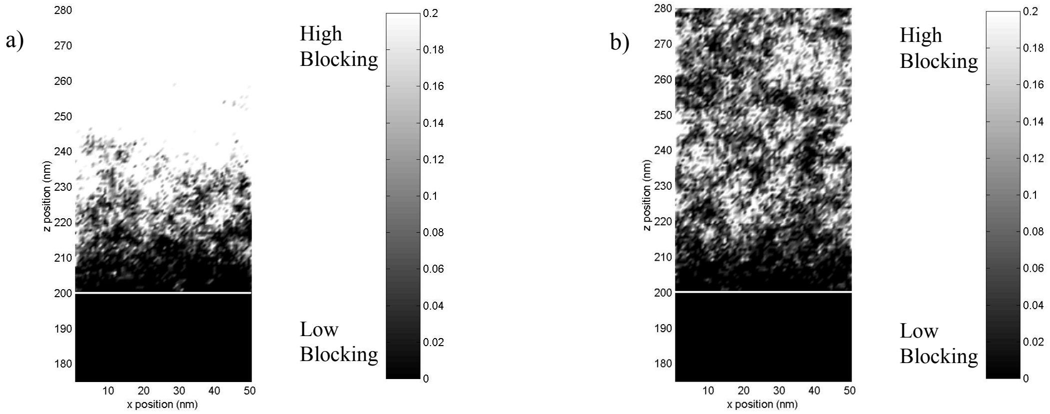

**Figure 8:** Simulation results for upper layer with a) no acid and b) upper layer with acid loading equivalent to 0.26 wt% PAG loading. White lines indicate position of the initial bilayer interface.

### 4.2 Reaction Depletion

Changing the initial blocking fraction of the upper layer can be used to simulate the reaction depletion effect. Figure 8a above can be consider the base case for the reaction depletion experiment. Figure 8a simulates diffusion into an 80% blocked upper layer. Figure 9a shows a sample with an upper layer 25% blocked prior to post exposure baking, while Figure 9b shows the resulting extent of deprotection after post exposure baking. The diffusion distance in Figure 9b is less than 10 nm. The estimate of diffusion distance obtained from IR analysis is approximately 10 nm for a 25% blocked film. For an 80% blocked film (as in Figure 8a) the IR measurement yields an estimated diffusion distance of 30 nm. Simulated results for both cases are within the experimental error of the IR measured values.

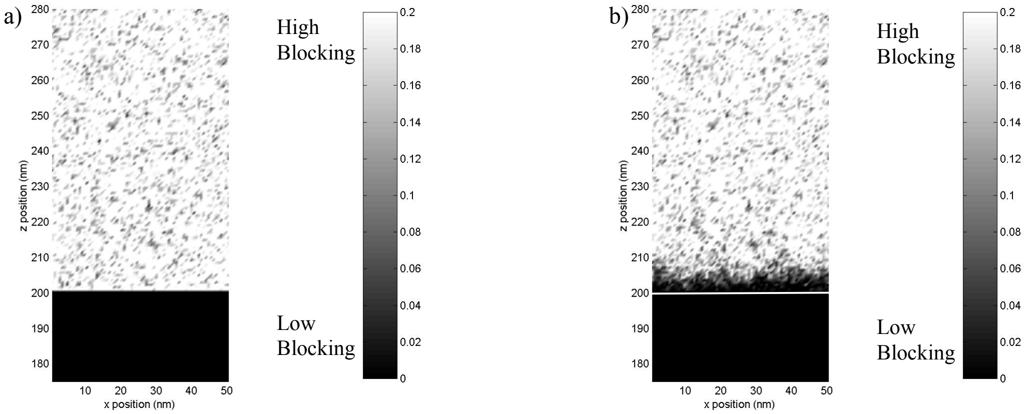

**Figure 9:** Simulation results of a partially blocked upper layer. Upper layer was 20% blocked. Initial condition is shown in 8a. Final condition is shown in 8b

## 5. CONCLUSIONS

Contributors to LES include aerial image formation, 2-D convergent diffusion at the line end, and the relative shallowness of the exposure gradient at the line end. Shortening in the aerial image results from operating near the resolution limit of the imaging system. Only by improving resolution of the imaging system can LES contributed by the aerial image be reduced. LES resulting from geometry effects cannot be avoided in positive-tone systems. At the line end in positive-tone systems diffusion will be convergent and photoproduct concentration will decrease more slowly than in the 1-D diffusion case present at the line edge. As a result, diffusion will be faster and thus farther over the course of a post exposure bake. In addition to the shape effect present at the line end, diffusion can also be affected by the exposure gradient present at the line end. Typically this gradient will be shallower at the line end than at the line edge. In a chemically amplified system transport occurs by a reaction-diffusion mechanism, which complicates simulation of the transport process. Two effects present in gradient diffusion were studied: the concentration enhancement effect and the reaction depletion effect. Experiments were designed to separate these to normally coupled effects. Simulation was then used to combine the diffusion effects. Our mesoscale post exposure bake model was found to generally capture the trend of these effects.

## REFERENCES

1. C. A. Mack, *Microlithography World*, **9-2**, 25-26 (Spring 2000)
2. C. A. Mack, *Microlithography World*, **9-4**, 25 (Autumn 2000)
3. X. Shi, B. Socha, J. Bendik, M. Dusa, W. Conley, B. Su, *Proc. SPIE*, **3678**, 777, (1999)
4. M. Cheng, E. Croffie, A. Neureuther, *Proc. SPIE*, **3678**, 867, (1999)
5. S.V. Postnikov, M.D. Stewart, H.V. Tran, M.A. Nierode, D.R. Medeiros, T. Cao, J. Byers, S.E. Webber, C.G. Willson, *J. Vac. Sci. Technol. B*. **17(6)**, 3335, (1999)
6. M. D. Stewart, M. H. Somervell, H. V. Tran, S. V. Postnikov, C. G. Willson, *Proc. SPIE*, **3999**, 665-674, (2000)
7. M.A. Zuniga, G.M. Wallraff, A.R. Neureuther, *Proc. SPIE*, **2438**, 113-124 (1995)
8. S.D. Burns, M.D. Stewart, J.N. Hilfiker, R.A. Synowicki, G.M. Schmid, C. Brodsky, C.G. Willson, “Determining free volume changes during the PEB and PAB of a chemically amplified resist”, *12th International Conference on Photopolymers*, Oct. 16 2000.
9. H. Ito, M. Sherwood, *Proc. SPIE*, **3678**, 104-115, (1999)
10. G.M. Schmid, V.K Singh, L.W. Flanagin, M.D. Stewart, S.D. Burns, C.G. Willson, *Proc SPIE,* **3999**, 675-685, (2000)
11. G.M Schmid, M.D. Smith, C.A. Mack, V.K. Singh, S.D. Burns, C.G. Willson, “Understanding molecular level effects during post exposure processing”, These Proceedings

## ACKNOWLEDGEMENTS

The authors gratefully acknowledge SRC and DARPA who provided financial support through Contract # LC-460. The authors would like to thank TriQuest Chemical Co. and Midori Kagaku, Co for providing valuable materials used in this work. The authors would also like to thank Dr. Chris A. Mack of KLA-Tencor (FINLE Division) for his generous donation of PROLITH™ simulation software to the Willson Research Group and for helpful discussions on the imaging aspects of line end shortening. Funding for M. Stewart was provided through a SRC/AMD Graduate Research Fellowship.